Efficient generation of graph states for quantum computation

S R Clark†, C Moura Alves†‡ and D Jaksch†

†Clarendon Laboratory, University of Oxford, Parks Road, Oxford OX1 3PU, U.K.
‡DAMTP, University of Cambridge, Wilberforce Road, Cambridge CB3 0WA, U.K.

E-mail: s.clark@physics.ox.ac.uk

Abstract. We present an entanglement generation scheme which allows arbitrary graph states to be efficiently created in a linear quantum register via an auxiliary entangling bus. The dynamics of the entangling bus is described by an effective non-interacting fermionic system undergoing mirror-inversion in which qubits, encoded as local fermionic modes, become entangled purely by Fermi statistics. We discuss a possible implementation using two species of neutral atoms stored in an optical lattice and find that the scheme is realistic in its requirements even in the presence of noise.

PACS numbers: 03.67.Mn, 03.67.Lx

1. Introduction

Bipartite entanglement has long been recognized as a useful physical resource for tasks such as quantum cryptography and quantum teleportation. Similarly, multipartite entanglement is an essential ingredient for more complex quantum information processing (QIP) tasks, and interest in this resource has grown since its controlled generation was demonstrated in several physical systems [1, 2, 3, 4, 5]. An important class of multipartite entangled states are graph states. By using vertices in a graph to represent qubits, and edges to represent an Ising type interaction that has taken place between two qubits, the graph formalism gives an intuitive characterization of entanglement by the presence of edges [6]. As a result a graph represents a preparation procedure for a state. Additionally graph theory allows some properties of these states, such as the effects of local Pauli operations and the persistence of entanglement after local Pauli measurements, to be computed exactly, and others, such as the Schmidt measure, which is computationally intractable for general states, to be bounded from above and below [7, 6]. The class of graph states includes many well studied states such as GHZ states, and special instances of graph states are the resource used in quantum error correcting codes [8, 9] and in one-way quantum computing [10, 11].

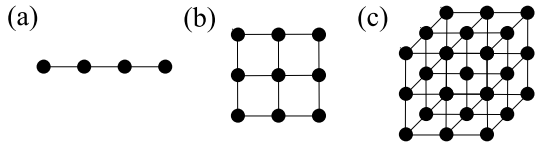

Figure 1. Examples of (a) 1D, (b) 2D and (c) 3D Cluster states. States (b) and (c) (and larger versions thereof) are a universal resource for one-way quantum computing.

Initial proposals for the generation of graph states in physical systems have focussed on qubit lattices of fixed geometry, where each qubit interacts only with its nearest-neighbors [6, 7, 11]. Such a scheme has been experimentally implemented in a three-dimensional (3D) optical lattice of neutral atoms via controlled collisions [1] along one axis of the lattice. The graph states generated with this method follow the geometry of the lattice, and so for collisions along one-axis an array of 1D cluster states, similar to figure 1(a), where obtained. Extending this process to all axes of 2D and 3D square lattices generates Cluster states of the form figure 1(b) and figure 1(c) respectively. These both constitute, together with single qubit measurements, a universal resource for quantum computation [10]. Despite the 1D Cluster states of the type shown in figure 1(a) not being a universal resource they are still a useful resource for specific computational tasks, as emphasized by the recent use of the four-qubit 1D Cluster state to implement the two-qubit Grover search algorithm with photons [3]. More generally the wider class of graph states also represent specific resources for certain QIP tasks, and this builds upon the notion that entanglement is an algorithmic resource [11]. The direct generation of more complex graphs, where the set of edges does not translate into

a regular arrangement of the underlying qubits, e.g. the quantum Fourier transform graph state [6], requires the ability to pre-engineer a complicated geometry of the qubit interactions. A simple scheme in which any graph state can be created in a set of qubits with a regular fixed geometry is therefore highly desirable. Some progress has been made towards this with non-deterministic linear optical protocols [12, 13] where proposals have been made for graph states generation in photon and solid-state qubits.

In this paper we propose a deterministic scheme for efficiently generating arbitrary graph states within a linear quantum register. We consider a general setup in which there is an auxiliary system, which we denote as an entangling bus (EB), running parallel and along the length of the register. All entanglement within the register is generated via the EB by performing local swaps between the subsets of register qubits and the EB and allowing the EB to evolve for a fixed time. More specifically the EB is an 'always on' 1D system whose dynamical evolution over a fixed time generates a specific entangling operation $\mathcal{C}$ composed of controlled-σ_z (c-σ_z) gates between all pairs of the transferred qubits in one step. After local swaps back to the register this operation allows arbitrary GHZ-type graph states [6] within the register qubits. There are three main results we present here based on this setup.

Our first result (i) is a construction of the EB using a 1D non-interacting fermionic lattice. Here qubits from the register become encoded as local fermionic modes (LFMs) [14]. We begin in section 2.1 by showing that for an engineered lattice with a specific spatially varying hopping profile the dynamical evolution over some fixed time results in the complete mirror inversion of the LFMs. This inversion is then shown to generate robust phases within the fermionic state purely as a consequence of Fermi statistics which are equivalent to entanglement between the LFM qubits resulting from an effective entangling operation $\mathcal{C}$ in section 2.2.

Our second result (ii) is then a scheme which utilizes the availability of the entangling operation $\mathcal{C}$ through the EB, with particular attention to the fermionic system in result (i), to efficiently generate arbitrary graph states within the register. Specifically we show that any graph state of n vertices can be generated in at most $O(2n)$ EB steps representing an improvement over the $O(n^2)$ steps required in a network model composed of two-qubit gates. In figure 2 the scheme is depicted for two-qubits.

In section 4 we present our third result (iii) which is a proposal for the implementation of this scheme in an optical lattice of neutral atoms. We begin in section 4.1 by examining how an effective XY spin chain can be engineered within an optical lattice. Two adjacent spin chains then form the basis of the register and EB. In section 4.2 we investigate how imperfections in the mapping of the optical lattice to an XY spin chain alter the fidelity of the EB dynamics. Finally, in section 4.3 we briefly note some other viable alternatives for implementing this scheme.

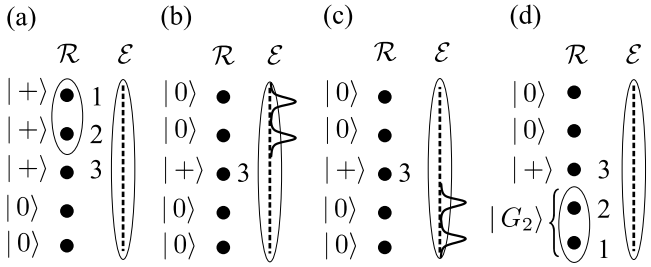

Figure 2. (a) Consider a quantum register $\mathcal{R}$ which has 3 graph qubits in a state $|+\rangle$. (b) Two of them are transferred to the EB $\mathcal{E}$ where their state is mapped into local fermionic modes. (c) $\mathcal{E}$ evolves via $H_{\rm f}$ for time τ, which results in the mirror-inversion of the two qubits. (d) The qubits at the mirror-inverted location are transferred back to $\mathcal{R}$, yielding a graph state with 2 vertices $|G_2\rangle$. Repeating this procedure with different qubits allows any 3-qubit graph state to be generated in $\mathcal{R}$.

2. Non-interacting fermionic system

2.1. Mirror inversion on a lattice

The construction of the fermionic EB relies on the fermionic system being *mapped* from another underlying system. The specific example we consider is a XY spin chain composed of N spins which is described by the Hamiltonian

$$H_{\rm XY} = \sum_{n=1}^{N-1} \lambda_n^z \sigma_n^z - \lambda_n^{xy}(\sigma_n^x \sigma_{n+1}^x + \sigma_n^y \sigma_{n+1}^y), \tag{1}$$

where λ_n^{xy} are the spatially varying XY couplings and λ_n^z is the contribution of an external field taken to be uniform as $\lambda_n^z = B/2$. It is well known that the Jordan Wigner transformation (JWT) [15] maps the XY spin chain to a non-interacting fermionic Hamiltonian

$$H_{\rm f} = -\sum_n j_n(c_n^\dagger c_{n+1} + c_{n+1}^\dagger c_n) + \sum_n u_n c_n^\dagger c_n, \tag{2}$$

where $j_n = 2\lambda_n^{xy}$, $u_n = B$, and c_n is a fermionic destruction operator for the nth site obeying the usual anticommutation relations. We are particularly interested in the *angular momentum* hopping profile [16] given by $j_n = (J/2)\sqrt{n(N-n)}$, with J a constant. We choose to write this as $j_n = W\alpha_n$ with $\alpha_n = 2\sqrt{(n/N)[1-(n/N)]}$ and $W = JN/4$. In this way the spatial dependence of the hopping j_n is contained entirely in the profile α_n obeying $0 < \alpha_n \leq 1$, and the overall scaling is given by the constant W such that $\max(j_n) \leq W$. With this hopping profile the projection of $H_{\rm f}$ onto the single fermion subspace of the lattice, $\mathcal{H}_1$, results in a Hamiltonian equivalent to $H_1 = -JS_x + B\mathbb{1}$, where S_x is the x-angular momentum operator for an 'effective' spin-$\mathcal{S}$ particle, with $\mathcal{S} = (N-1)/2$. The single-fermion states $\{|\,n\rangle = c_n^\dagger\,|\,\text{vac}\rangle\}$ then correspond to the z-angular momentum eigenstates $\{|\,\mathcal{S}, l\rangle_z\}$ of the spin-$\mathcal{S}$ particle, with $|\,1\rangle = |\,\mathcal{S}, -\mathcal{S}\rangle_z, \ldots, |\,N\rangle = |\,\mathcal{S}, \mathcal{S}\rangle_z$. The dynamics generated in $\mathcal{H}_1$, when H_1 is applied for a fixed time $\tau = \pi/J$, result in the time-evolution unitary

$U_1(\tau) = \exp(i\phi_B)\exp(i\pi S_x)$ composed of an overall phase $\phi_B = -B\pi/J$ for $\mathcal{H}_1$ and a rotation of the spin-$\mathcal{S}$ particle about the x-axis by π. This leads directly to perfect state transfer over the lattice [16].

The action of $U_1(\tau)$ on the single-particle basis follows from its equivalence to the z-angular momentum states where $\exp(i\pi S_x)\,|\,\mathcal{S}, l\rangle_z = \exp(i\pi\mathcal{S})\,|\,\mathcal{S}, -l\rangle_z$. Thus we find that $U_1(\tau)\,|\,n\rangle = \exp(i\phi_1)\,|\,\bar{n}\rangle$, with the phase $\phi_1 = \pi\mathcal{S} + \phi_B$ and mirror-conjugate location $\bar{n} = N - n + 1$. The choice $B = \mathcal{S}J$ then ensures that the single-particle phase ϕ_1 vanishes. The evolution of the fermionic modes $c_n^\dagger$ can then immediately be seen to satisfy $Uc_n^\dagger U^\dagger = c_{\bar{n}}^\dagger$, where $U = \exp(-iH_{\mathrm{f}}\tau)$, with respects to the full Hamiltonian H_{f}, and the dynamics of the system describes the complete mirror-inversion of the LFMs. Typically implementations of this effective fermionic system will have a maximum obtainable value for the over scaling W of the hopping which prevents J from being arbitrarily increased, and so once it is maximized we must pay a linear cost in the inversion time τ with the increasing size of the system N.

2.2. Entanglement of fermionic modes

Under the JWT the N qubit (or spin) states $|\,q_1, \ldots, q_N\rangle$, with $q_n \in \{0, 1\}$, of the chain are mapped to Fock states of the LFMs as $|\,q_1, \ldots, q_N\rangle = (c_1^\dagger)^{q_1} \ldots (c_N^\dagger)^{q_N}\,|\,\mathrm{vac}\rangle$ (where operators are ordered according to the lattice) which describe the occupancy of the system by quasi-fermions. The use of fermionic mode occupancy as a basis for quantum computation has been proposed before [14]. An immediate difficulty with a direct implementation of this approach using massive and/or charged fermions is the constraint caused by *superselection* rules which prohibits the superposition of states with different mass/charge eigenvalues [17, 18]. Such superpositions are essential for our LFM qubit encoding. In [14] the accessibility of the Fock space is widened by including an interaction with a superconductor reservoir that relaxes particle number conservation to pairs. Also, in contrast to bosons, the Fock space of fermions does not have a natural tensor product structure permitting independent operations on each mode [19]. This intrinsically nonlocal behavior of fermions adds a significant degree of complexity to quantum computing with LFM qubits in [14]. Here, in contrast, we have focussed on a physical system which *maps* to a non-interacting fermionic system. As a result the quasi-Fock space is fully accessible, thus enabling superpositions of states with different numbers of quasi-fermions, which are essential for encoding qubits.

For systems of identical fermions a bilinear fermionic Hamiltonian such as H_{f} suffices to generate mode entanglement, despite describing a non-interacting system [20]. This is a natural consequence of the nonlocal character of fermions. The entanglement generated by mirror-inversion then follows straightforwardly from Fermi statistics through its action on Fock states as

$$e^{-iH_{\mathrm{f}}\tau}\,|\,q_1, \ldots, q_N\rangle = e^{-i\pi\Sigma_Q}\,|\,q_N, \ldots, q_1\rangle\,, \tag{3}$$

where Σ_Q is the number of anti-commutations of the operators $c_n^\dagger$ required to reestablish a Fock state. Specifically $\Sigma_Q = Q(Q-1)/2$, where Q is the number of fermions, i.e.

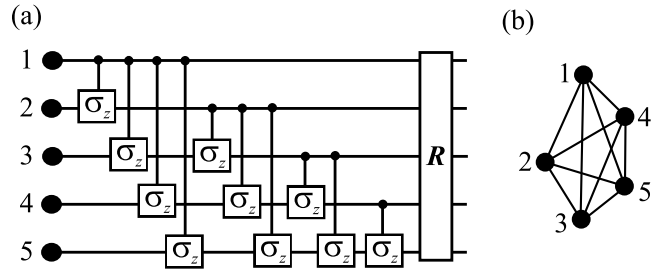

Figure 3. For 5 qubits we have (a) the quantum circuit $\mathcal{C}(5)$ equivalent to the dynamics of $H_{\rm f}$ for a time τ, and (b) the fully connected graph state $|G_5\rangle$ with 5 vertices generated by this circuit if all the qubits are initialized in the $|+\rangle$ state. Both the circuit and the resulting graph state generalize in an obvious way for more qubits.

$Q = \sum_{n=1}^{N} c_n^\dagger c_n = \sum_{n=1}^{N} q_n$, and so phases are only acquired between subspaces with different Q. Since equation (3) is written in terms of Fock states, the inverse-JWT removes the implied antisymmetry when mapping back to qubits, while leaving the phases acquired between fermion-number (or total magnetization) subspaces untouched. Thus the evolution of the EB after a fixed time τ is equivalent to a quantum circuit $\mathcal{C}(N)$ composed of c-σ_z gates between all distinct pairs of N qubits followed by the inversion operator R, as shown in figure 3(a) for $N = 5$. Usefully, if any $N - q$ qubits of the system are in the state $|0\rangle$, then this circuit reduces to $\mathcal{C}(q)$ between the remaining q qubits, independent of their locations, followed by the full inversion R of all qubits.

2.3. Generalizations

In passing we note that the above results apply to more general settings. Suppose we partition the fermionic lattice into M equal blocks, each labelled by their central site k, and composed of sites $m(k)$. Within each block k we consider an extended fermionic mode $f_k^\dagger = \sum_{n\in m(k)} \phi_n^k c_n^\dagger$, defined by a single-particle state ϕ_n^k contained entirely within the block k and symmetrical about its center. The dynamics of the EB over some fixed time will be equivalent to $\mathcal{C}(M)$ R as long as j_n and u_n are chosen such that the dynamics of $H_{\rm f}$ performs mirror-inversion with respect to the modes $f_k^\dagger$ [21, 22]. We can equally consider partitioning a 1D continuous fermionic system, described by field operators $\hat{\psi}^\dagger(x)$, and defining extended LFMs analogously as $f_k^\dagger = \int_{m(k)} dx\ \phi^k(x)\hat{\psi}^\dagger(x)$, via a single-particle wavefunction $\phi^k(x) = 0$, $\forall\, x \notin m(k)$. In this case harmonic trapping $V(x) = m\omega^2 x^2/2$ and Gaussian wavefunctions $\phi^k(x)$ centered on a block are sufficient for mirror-inversion over a time $\tau = \pi/\omega$. Such an arrangement could potentially be implemented using effective bosonic Fock states of arrays of atomic quantum dots [23] following conceptually similar lines to the 1D cold-collision proposal in [24], but with the difference that the Tonks-Girardeau limit [25] of the bosons is exploited to yield an effective non-interacting fermionic system.

3. Entanglement generation scheme

To utilize the EB for the generation of arbitrary graph states we require it to be augmented with a linear register of N qubits for storage. As with other such schemes each qubit in the register is assumed to be individually manipulable and measurable. This includes the ability for each qubit to be selected to undergo a transfer process which maps its state into a LFM encoded qubit in the EB via $\sigma_n^+ \mapsto c_n^\dagger$, where σ_n^+ is the Pauli ladder operator on the register. Since the register is a distinct commuting physical system to the EB the transfer process allows certain sets of qubits to be temporarily endowed with fermionic character and subsequently become entangled as a result of the mirror-inversion.

The register and the EB are taken to be initialized in the states $\otimes_i^N |\,0\rangle_i$ and $|\,\mathrm{vac}\rangle$ respectively. The scheme begins by choosing a set of register qubits Γ to be the graph vertices, and applying a Hadamard transformation to each of them: $|\,0\rangle \rightarrow |\,+\rangle = (|\,0\rangle + |\,1\rangle)/\sqrt{2}$, as in figure 3(a) for qubits $1-3$. A subset Σ of m of these qubits is then transferred to the EB and allowed to evolve for a time τ, as shown (for $m = 2$) in figure 3(b) and figure 3(c) for qubits 1 and 2. The qubits encoded by LFM at the corresponding mirror-inverted locations $\bar{\Sigma}$ of the EB are then transferred back to the register, yielding a fully connected graph state $|\,G_m\rangle$ between these m vertices, as in figure 3(d). Such a state is locally equivalent to a m-qubit GHZ state, as depicted in figure 3(b) for $m = 5$. Overlap between EB and register graph qubits after inversion has occurred can be avoided by choosing $|\Gamma| = \lceil N/2 \rceil$ with locations in the first half of the register.

This setup can generate any graph state of n vertices in at most $O(n^2)$ steps by utilizing only the two-qubit interaction of the EB to establish each edge individually, mimicking a network model of two-qubit gates. However, by exploiting the multi-qubit circuit implemented by the EB dynamics over the same time τ, as in figure 3(a), our scheme can improve this upper bound. Specifically, we proceed iteratively, starting with $g = 1$, by :

(i) transferring the gth graph qubit, and all graph qubits $g_c > g$ which will connect to g, into the EB;

(ii) allowing them to evolve for a time τ creating a complete set of connections between these vertices, c.f. figure 3(b);

(iii) then transferring qubit g back to the register while leaving the qubits g_c to evolve for one cycle longer in the EB, subsequently removing all the connections between them;

(iv) finally transferring the qubits g_c back to the register and repeating step (i) with $g \mapsto g + 1$.

Thus, any graph of $g = n$ vertices can be generated in at most $O(2n)$ uses of the EB.

4. Implementations

4.1. Optical lattice realization

The physical basis for the implementation of the scheme which we focus on is an optical lattice of ultracold bosonic atoms [26]. In an optical lattice neutral atoms are trapped due to the optical dipole force in the intensity maxima (or minima) of a far-off resonance standing wave light-field formed from counter-propagating lasers. We consider atoms possessing two long-lived internal (hyperfine) states $|\,a\rangle$ and $|\,b\rangle$ which are trapped by two such optical lattices of different polarizations. For sufficiently low temperatures and deep lattices the atoms become restricted to the lowest Bloch band and their dynamic over a system of N sites is described by a two-species Bose-Hubbard model (BHM) given by [27]

$$H = \sum_{n=1}^{N}\left(\frac{U_n^a}{2}a_n^{\dagger 2}a_n^2 + \frac{U_n^b}{2}b_n^{\dagger 2}b_n^2 + U_n^{ab}a_n^\dagger a_n b_n^\dagger b_n\right) - \sum_{n=1}^{N-1}\left(t_n^a a_n^\dagger a_{n+1} + t_n^b b_n^\dagger b_{n+1} + \text{H.c.}\right) + H_B, \tag{4}$$

where $a_n(b_n)$ is the bosonic destruction operator for an $a(b)$-atom in the nth site, and $H_B = (B/2)\sum_n(a_n^\dagger a_n - b_n^\dagger b_n)$ is the contribution of an external field which we assume to be uniform over the system. The parameters $t^{a(b)}$ and $U^{a(b)}$, U^{ab} are the laser-intensity-dependent hopping matrix elements and on-site interactions for atoms in states $|\,a\rangle$ ($|\,b\rangle$) respectively. These parameters will in general have a spatial profile across the lattice. The dynamic controllability and long decoherence times of this system have made it of considerable interest for QIP [28, 29] and for realizing spin models [27, 30].

The scheme requires an initial state with one atom per site (each in a state $|\,a\rangle$) and single site addressability for manipulations and ultimately for imaging also. While the preparation of a high-fidelity initial state could be achieved using the techniques described in [31, 32], single site addressability remains a challenging technical limitation in optical lattices. However, there are theoretical proposals which offer the potential to overcome this by using ideas such as marker atoms to localize global operations [33], as well as increasing technical improvements seen in experiments. Here we assume single-site addressability and consider it as being implemented by a laser with a Gaussian waist on the order of the size of a single site.

Initially we take the lattice as being sufficiently deep to prohibit hopping in all directions. A chain of sites from the commensurately filled lattice is then selected to be the register of non-interacting qubits. An adjacent chain then represents the EB. Addressability is then exploited again to engineer a spatially dependent intensity profile along the EB chain which activates hopping exclusively along this chain. The transfer process between the register and EB is then accomplished by again using addressability to localize Raman induced hopping [26] between two adjacent register and EB sites and implement a swap gate, as described in detail in [28], on a timescale sufficiently faster than τ.

For the non-zero hopping within the EB chain we focus on the two-species BHM in the limit of large interactions, $U^a, U^b, U^{ab} \gg t^a, t^b$, which energetically prohibit the multiple occupancy of any site. The hopping can be then treated perturbatively and to lowest order, for an initial Mott insulating state with commensurate filling of one atom per lattice site, the effective Hamiltonian is found to be [27]

$$H_{\rm S} = \sum_{n=1}^{N-1} \lambda_n^{zz}\sigma_n^z\sigma_{n+1}^z + \lambda_n^z\sigma_n^z - \lambda_n^{xy}(\sigma_n^x\sigma_{n+1}^x + \sigma_n^y\sigma_{n+1}^y). \tag{5}$$

Hence we obtain the anisotropic Heisenberg spin model in the optical lattice, with the correspondence $|\,a\rangle \equiv |\uparrow\rangle$ and $|\,b\rangle \equiv |\downarrow\rangle$ at each site. The corresponding Pauli operators are then $\sigma_n^z = a_n^\dagger a_n - b_n^\dagger b_n$, $\sigma_n^x = a_n^\dagger b_n + b_n^\dagger a_n$, $\sigma_n^y = -i(a_n^\dagger b_n - b_n^\dagger a_n)$, while the couplings are given by

$$\begin{aligned}
\lambda_n^{zz} &= \frac{t_n^{a2} + t_n^{b2}}{2U_n^{ab}} - \frac{t_n^{a2}}{U_n^a} - \frac{t_n^{b2}}{U_n^b} \\
\lambda_n^{xy} &= \frac{t_n^a t_n^b}{U_n^{ab}} \\
\lambda_n^z &= 4\left(\frac{t_n^{a2}}{U_n^a} - \frac{t_n^{b2}}{U_n^b}\right) + \frac{B}{2}.
\end{aligned} \tag{6}$$

The construction of the EB requires the optical lattice parameters to be engineered such that $U_n^a = U_n^b = 2U_n^{ab}$ and $t_n^a = t_n^b$, thereby ensuring that $\lambda_n^{zz} = 0$, $\lambda_n^z = B/2$, and that $H_{\rm S}$ reduces to the pure XY spin chain Hamiltonian $H_{\rm XY}$.

The spatial dependence of the two-species BHM model parameters arise due to some appropriately configured laser-intensity profile along the system. Since the on-site interactions have a weak dependence on the laser-intensity, in contrast to hopping matrix elements which have an exponential dependence [26], only hopping is assumed to be spatially dependent over the system. Specifically, we take $t_n^a = t_n^b = T\sqrt{\alpha_n}$, where the spatial dependence is again contained in the profile α_n, and the overall scaling is given by a constant T such that $\max(t_n^{a(b)}) \leq T$. The interaction energies are constant over the system and defined as $U^a = U^b = 2U^{ab} = U$. To first order in T/U the dynamics of the optical lattice reduces to an XY spin chain with couplings $\lambda_n^{xy} = (2T^2/U)\alpha_n$. The profile α_n must then have the spatial dependence introduced earlier in section 2.1 enabling the effective non-interacting fermionic lattice resulting from this XY spin chain to undergo mirror-inversion. This dynamical evolution will proceed exactly in the ideal limit where $U/T \gg 1$. The graph states generated with this implementation could then be used for one-way quantum computation if single site imaging was available, or alternatively the multi-qubit entanglement could be diagnosed with the procedure described in [34].

4.2. Optical lattice imperfections

We have considered some dominant sources of imperfections within the optical lattice implementation of the EB. In particular, we investigated the fidelity of the two-species BHM to spin-chain mapping introduced earlier, for finite U/T. We considered a system

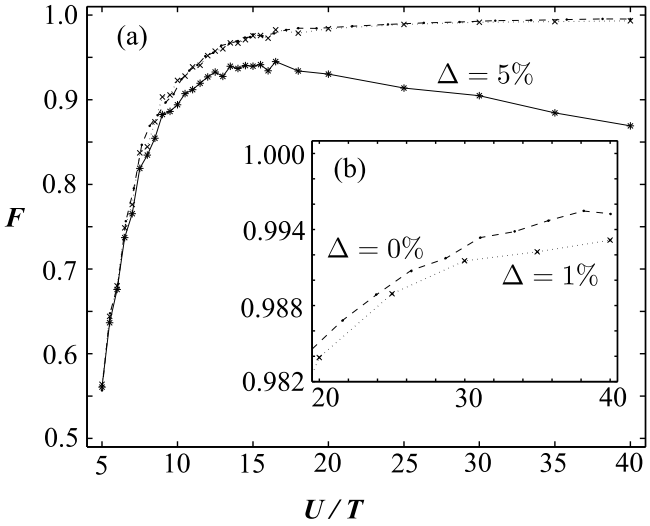

Figure 4. (a) The fidelity F of the effective XY spin-chain implemented by the 2-species BHM with the ratio U/T, for no noise $\Delta = 0\%$ ($\cdot$), $\Delta = 1\%$ ($\times$) and $\Delta = 5\%$ ($*$). (b) A close-up of (a). The solid, dashed and dotted lines are drawn to guide the eye.

of size $N = 6$ initialized in a product state $|+\rangle \otimes |0\rangle^{\otimes 4} \otimes |+\rangle$, and computed the exact time-evolution of the two-species BHM, using the time-evolving block decimation (TEBD) algorithm [35, 36], for varying U/T over the appropriate inversion time τ. Using the effective two-spin density matrix for the end sites, the fidelity F was computed with the state $|G_2\rangle$ obtained from a perfectly implemented XY chain. The simulation results in figure 4(a) demonstrate that, as expected, the fidelity increases with U/T. Given that $\tau = UN\pi/16T^2$, the increasing the fidelity, induced by deepening the lattice, comes at the cost of longer inversion times. However, figure 4(b) shows that $F > 0.99$ even at a moderate ratio of $U/T = 26$, and we found this curve to be largely independent of N for $N \sim O(10)$ tested. At this depth a $\lambda = 514$ nm optical lattice of ^{23}Na atoms has $\tau = 9.3$ ms, while a $\lambda = 826$ nm optical lattice of ^{87}Rb atoms has $\tau = 79$ ms. These are fast enough for multiple EB inversions to occur within the decoherence time of the system, which is typically of order of a second [37, 38].

We have also investigated the effect of jitter in the lattice laser intensities. For ^{87}Rb the laser intensities I_a and I_b of the a and b lattices were taken as varying independently according to some Wiener noise $dW_{a(b)}(t)$ with variance Δ^2: $I_{a(b)}(t) = I_0 + dW_{a(b)}(t)$, where I_0 is the ideal laser intensity. Such laser fluctuations are then nonlinearly related to the corresponding fluctuations in the hopping $t_n^{a(b)}$ and on-site interaction $U^{a(b)}, U^{ab}$ matrix elements of the 2-species BHM [26]. We assumed a simplified version of this noise in which the intensity fluctuations alter, according to these nonlinear relations, the hopping and interaction scalings T and U contained within the overall scaling W of j_n, but not the spatial profile α_n. Despite this restriction, this noise causes fluctuations in the inversion time τ during the dynamics, and also breaks the symmetry required to

ensure that no $\sigma_n^z\sigma_{n+1}^z$ or spatially-varying σ_n^z contributions occur. In figure 4(a) the fidelity curves are plotted for $\Delta = 1\%$ and $\Delta = 5\%$ of I_0. For $\Delta = 5\%$ the fidelity is seen to drop off in deeper lattices due to the cumulative effect of noise over longer inversion times. Crucially, the fidelity curve suffers only a minimal reduction due to $\Delta = 1\%$ noise, as in figure 4(b), and this represents a realistic value for the experimental stabilization of the laser intensity.

4.3. Alternative implementations

Finally, we note that the scheme described in section 3 could be implemented in any physical system where the entangling operation $\mathcal{C}$ is available. Specifically the architecture composed of a register and EB considered here could in principle be implemented in any system where adjacent engineered spin-chains are realizable. This requirement is particularly well suited to solid state systems such as arrays of quantum dots with one electron per dot in an external magnetic field [39, 40]. Here the qubit is encoded in the spin degree of freedom of the electron and the dynamics are described by a standard Heisenberg Hamiltonian. The presence of $\sigma_n^z\sigma_{n+1}^z$ terms in this Hamiltonian can be compensated by an appropriate spatially varying external magnetic field [16], while the angular momentum coupling profile can then be produced by controlling the external voltage applied to the gates defining the tunnelling barriers between the dots. However, such an implementation is currently limited by the small numbers of solid-state qubits realizable.

Another possibility is trapped ions [41]. A scheme for generating GHZ-type states over a chain of many ions has been proposed [42] and experimentally realized for four-qubits [4]. Although implemented by different means the entangling procedure in [42] is locally equivalent to the entangling operation $\mathcal{C}$ when applied globally to the entire register. Permitting single-ion addressability, which has also been experimentally demonstrated [43], allows universal two-qubit quantum gates to be implemented by the same method [44], and additionally by addressing many ions $\mathcal{C}$ can be applied to any subset of qubits. Thus the entangling operation constructed above for optical lattices via the EB is also realizable in ion trap systems via the collective vibrational degrees of freedom of the ions.

5. Conclusions

We have shown how arbitrary Graph states can be generated efficiently by using an EB whose dynamics correspond to a non-interacting fermionic system undergoing mirror-inversion. By utilizing an EB which is fixed and always on the dynamical control required for QIP tasks can be reduced to single qubit operations. Here an implementation of this scheme using an optical lattice of neutral atoms was considered in detail. The fidelity of the optical lattice proposal was examined not only for the depth ratio U/T, but also in the presence of noise, and found to be both realistic and robust. We have also briefly

noted the suitability of the scheme to other physical systems.

Acknowledgments

This work was supported by the EPSRC IRC network on Quantum Information Processing (U.K.). S.C. and D.J. thank Peter Zoller and Hans Briegel for stimulating discussions. C.M.A. thanks Marc Hein for insightful discussions on graph states and is supported by the Fundação para a Ciência e Tecnologia (Portugal).

References

[1] Mandel O, Greiner M, Widera A, Rom T, Hänsch T W and Bloch I 2003 *Nature* **425** 937
[2] Walther P, Pan J W, Aspelmeyer M, Ursin R, Gasparoni S, Zeilinger A 2004 *Nature* **429** 158
[3] Walther P, Resch K J, Rudolph T, Schenck E, Weinfurter H, Vedral V, Aspelmeyer M, Zeilinger A 2005 *Nature* **434** 169
[4] Sackett C A, Kielpinski D, King B E, Langer C, Meyer V, Myatt C J, Rowe M, Turchette Q A, Itan W M, Wineland D J, Monroe C 2000 *Nature* **404** 256
[5] Rauschenbeutel A, Nogues G, Osnaghi S, Bertet P, Brune M, Raimond J M and Haroche S 2000 *Science* **288** 2024
[6] Hein M, Eisert J and Briegel H J 2004 *Phys. Rev.* A **69** 062311
[7] Briegel H J and Raussendorf R 2001 *Phys. Rev. Lett.* **86** 910
[8] Gottesman D 1997 *Ph.D thesis* (CalTech, Pasadena)
[9] Steane A M 1996 *Phys. Rev. Lett.* **77** 793
[10] Raussendorf R and Briegel H J 2001 *Phys. Rev. Lett.* **86** 5188
[11] Raussendorf R, Browne D E and Briegel H J 2003 *Phys. Rev.* A **68** 022312
[12] Browne D E and Rudolph T 2004 *Preprint* quant-ph/0405157
[13] Barrett S D and Kok P 2004 *Preprint* quant-ph/0408040.
[14] Bravyi S B and Kitaev A Y 2002 *Ann. Phys.* **298** 210
[15] Sachdev S 2001 *Quantum Phase Transitions* (Cambridge Univ. Press, Cambridge).
[16] Christandl M, Datta N, Ekert A and Landahl A J 2004 *Phys. Rev. Lett.* **92** 187902
[17] Zanardi P 2002 *Phys. Rev.* A **65** 042101
[18] Zanardi P and Wang X 2002 *J. Phys. A: Math. Gen.* **35** 7947
[19] Wu L A and Lidar D A 2002 *J. Math. Phys.* **43** 4506
[20] Vedral V 2003 *Central Eur. J. Phys.* **1** 289
[21] Yung M H and Bose S 2004 *Quan. Inf. & Comp.* **4** 174
[22] Yung M H and Bose S 2005 *Phys. Rev.* A **71** 032310
[23] Recati A, Fedichev P O, Zwerger W, von Delft J, Zoller P 2005 *Phys. Rev. Lett.* **94** 040404
[24] Calarco T, Hinds E A, Jaksch D, Schmiedmayer J, Cirac J I and Zoller P 2000 *Fortschritte der Physik* **48** 945
[25] Paredes B, Widera A, Murg V, Mandel O, Fölling S, Cirac J I, Shlyapnikov G V, Hänsch T W and Bloch I 2004 *Nature* **429** 277
[26] Jaksch D, Bruder C, Cirac J I, Gardiner C W and Zoller P 1998 *Phys. Rev. Lett.* **81** 3108
[27] Duan L M, Demler E and Lukin M D 2003 *Phys. Rev. Lett.* **91** 090402
[28] Pachos J K and Knight P L 2003 *Phys. Rev. Lett.* **91** 107902
[29] Jaksch D and Zoller P 2004 *Ann. Phys.* **315** 52
[30] García-Ripoll J J and Cirac J I 2003 *New J. Phys.* **5** 76.1
[31] Griessner A, Daley A J, Jaksch J, Zoller P 2005 *Preprint* quant-ph/0502171
[32] Rabl P, Daley A J, Fedichev P O, Cirac J I, Zoller P 2003 *Phys. Rev. Lett.* **91** 110403
[33] Calarco T, Dorner U, Julienne P, Williams C, Zoller P 2004 *Phys. Rev.* A **70** 012306

[34] Moura Alves C and Jaksch D 2004 *Phys. Rev. Lett.* **93** 110501
[35] Vidal G 2003 *Phys. Rev. Lett.* **91** 147902
[36] Vidal G 2004 *Phys. Rev. Lett.* **93** 040502
[37] Greiner M, Mandel O, Esslinger T, Hänsch T W and Bloch I 2002 *Nature* **415** 39
[38] Hensinger W K, Häffner H, Browaeys A, Heckenberg N R, Helmerson K, McKenzie C, Milburn G J, Phillips W D, Rolston S L, Rubinsztein-Dunlop H, Upcroft B 2001 *Nature* **412** 52
[39] Golovach V N, Loss D 2002 *Semicond. Sci. Technol.* **17** 355
[40] Pashkin Y A, Yamamoto T, Astafiev O, Nakamura Y, Averin D V, Tsai J S 2003 *Nature* **421** 823
[41] Cirac J I, Zoller P 1995 *Phys. Rev. Lett.* **74** 4091
[42] Mølmer K, Sørensen S 1999 *Phys. Rev. Lett.* **82** 1835
[43] Roos C, Riebe M, Häffner H, Hänsel W, Benhelm J, Lancaster G P T, Becher C, Schmidt-Kaler F, Blatt R 2004 *Science* **304** 1478
[44] Sørensen S, Mølmer K 1999 *Phys. Rev. Lett.* **82** 1971